The flow of the Antarctic Circumpolar Current over the North Scotia Ridge

Inga J. Smith [a,b,*]
David P. Stevens [c]
Karen J. Heywood [a]
Michael P. Meredith [d]

[a] *School of Environmental Sciences, University of East Anglia, Norwich NR4 7TJ, U.K.*

[b] *Present address: Department of Physics, University of Otago, P.O. Box 56, Dunedin, New Zealand*

[c] *School of Mathematics, University of East Anglia, Norwich NR4 7TJ, U.K.*

[d] *British Antarctic Survey, High Cross, Madingley Road, Cambridge CB3 0ET, U.K.*

Abstract

The transports associated with the Subantarctic Front (SAF) and the Polar Front (PF) account for the majority of the volume transport of the Antarctic Circumpolar Current (ACC). After passing through Drake Passage, the SAF and the PF veer northward over the steep topography of the North Scotia Ridge. Interaction of the ACC with the North Scotia Ridge influences the sources of the Malvinas Current. This ridge is a major obstacle to the flow of deep water, with the majority of the deep water passing through the 3100 m deep gap in the ridge known as Shag Rocks Passage. Volume transports associated with these fronts were measured during the North Scotia Ridge Overflow Project, which included the first extensive hydrographic survey of the ridge, carried out in April and May 2003. The total net volume transport northward over the ridge was found to be 117 ± 10 Sv ($1\ \text{Sv}=10^6\ \text{m}^3\text{s}^{-1}$). The total net transport associated with the SAF was approximately 52 ± 4 Sv, and the total transport associated with the PF was approximately 58 ± 5 Sv. Weddell Sea Deep Water was not detected passing through Shag Rocks Passage, contrary to some previous inferences.

Key words:
Antarctic Circumpolar Current, Antarctic Polar Front, Subantarctic Front, volume transport, South Atlantic Ocean, North Scotia Ridge, Shag Rocks Passage
PACS: 92.10.Ty, 92.10.Dh

Personal revised version of: Deep-Sea Research I, 57, 14-28, doi:10.1016/j.dsr.2009.10.010.

1 Introduction

The Antarctic Circumpolar Current (ACC) is primarily a wind driven current that flows eastward around Antarctica, connecting the basins of the Pacific, Atlantic, and Indian Oceans. This connection allows the transfer of mass and heat between the oceans, and understanding these transfer processes is a crucial aspect of current climate research. In particular, inter-annual variability of the transport of the ACC is a priority for climate change monitoring programmes, while characterisation of typical transports of the ACC is important for the validation of climate models. Drake Passage, between the Antarctic Peninsula and the southern tip of South America, is often considered an ideal location to measure the transport of the ACC because of the latitudinal constriction of the flow of the ACC that occurs there. However, the major topographic constriction to the flow of the ACC is the North Scotia Ridge.

The ACC exists as a series of narrow fronts of fast flowing water with relatively quiescent water between the fronts (Orsi et al., 1995). The fronts are often vertically coherent, with strong velocities reaching to the seabed (Sun and Watts, 2001). The location of the fronts can have important implications for the ecology of the region, since they act as a barrier to genetic dispersal of some species (Shaw et al., 2004), and can provide pathways for the transport of others (Thorpe et al., 2004).

The bulk of the flow of the ACC is associated with two fronts, the Subantarctic Front (SAF) and the Polar Front (PF), with the remaining volume transport being associated either with the Southern ACC Front (SACCF) or with the areas between and adjacent to the fronts. The area equatorward of the SAF is referred to as the Subantarctic Zone (SAZ), the region between the SAF and PF as the Polar Frontal Zone (PFZ), and the area poleward of the PF as the Antarctic Zone (AAZ). A transect across Drake Passage is usually conducted annually along the line denoted as WOCE SR1b (Cunningham et al., 2003). The SR1b path was chosen by the WOCE Hydrographic Program to closely correspond with the track of the ERS-1 and 2 satellites (García et al., 2002), and runs between Burdwood Bank and Elephant Island. Cunningham et al. (2003), reanalysing the work of Whitworth and Peterson (1985) and Whitworth (1983), calculated the long term mean net volume transport of the ACC through Drake Passage to be 134 Sv, with a standard deviation of 11.2 Sv and error estimates of between 15 and 27 Sv. After exiting Drake Passage, the ACC flows through the Scotia Sea.

The North Scotia Ridge is an arc that runs for approximately 2000 km between Tierra del Fuego, at the southern tip of South America, and the island of

* Corresponding author. Fax: +64 (0)3 4790964
Email address: inga@physics.otago.ac.nz (Inga J. Smith).

South Georgia. This paper presents results from a cruise along approximately 1200 km of the North Scotia Ridge (Fig. 1). Only two fronts are observed crossing the North Scotia Ridge, with the remainder of the ACC transport forced to flow south of South Georgia. Whereas Drake Passage restricts the horizontal extent of the ACC, the North Scotia Ridge constrains the vertical structure of the ACC, since it forms a barrier to the northward flow of the deep water components. The western edge of the ridge is shallow, with typical depths along Burdwood Bank of 200 m. The ridge has a steep southern edge. Water depths along the crest of the ridge typically range from around 200 m to 2000 m (Fig. 1). The exception to this is Shag Rocks Passage, a 3100 m deep gap in the North Scotia Ridge, lying at approximately 53°S, 48°W, roughly 450 km west of Shag Rocks. This gap was identified, but not named, by Deacon (1933) from the charts of Herdman (1932). Crossing the North Scotia Ridge, the paths of the SAF and PF are strongly constrained by the bathymetry, with very little variation in their observed locations, a fact referred to in the literature at least as far back as Deacon (1933). However, Mackintosh (1946) noted some variation in the position of the surface position of the PF, then known as the Antarctic Convergence.

The SAF and PF cross the North Scotia Ridge, while the SACCF follows an eastward path to the south of South Georgia. Flows of the ACC across the Scotia Sea boundaries were examined by Naveira Garabato et al. (2002, 2003) reporting results from the 1999 cruise known as ALBATROSS (Antarctic Large-scale Box Analysis and the Role of the Scotia Sea). However, that cruise did not survey the North Scotia Ridge, so that transports associated with the fronts over the ridge could only be inferred indirectly. Naveira Garabato et al. (2003), using inverse modelling techniques to analyse measurements enclosing the Scotia Sea, deduced that the transport associated with the overflow of waters over the North Scotia Ridge and into the Georgia and Argentine Basins was 119±12 Sv. An estimate of 68±10 Sv was given by Arhan et al. (2002) for the transport of the PF through Shag Rocks Passage. In addition, Arhan et al. (2002) observed a transport of 14±11 Sv east of 40°15′W, which was attributed to a flow of water from the poleward side of the PF in the Scotia Sea over the North Scotia Ridge.

From satellite images of sea surface temperature (SST), Moore et al. (1997) noted that the SAF crosses the North Scotia Ridge east of Burdwood Bank, through a passage that will be referred to as the 54–54 Passage, since the passage lies at approximately 54°S, 54°W. The PF has been repeatedly observed within Shag Rocks Passage (Gordon et al., 1977). However, all previous studies have been over a large geographic scale, with consequently sparse data sets, or from remote sensing.

Examination of water mass transports upstream and downstream of the North Scotia Ridge by Naveira Garabato et al. (2003) indicated that an exchange

of water masses across the SAF and PF had occurred. A key objective of this current project was to examine if this was caused by the interaction of the fronts with the North Scotia Ridge. Table 1 shows the neutral density classes used by Naveira Garabato et al. (2002) to delineate water masses, based on work by Reid et al. (1977), Sievers and Nowlin (1984), and Arhan et al. (1999). The same classifications will be adopted in this paper to facilitate comparisons. Subantarctic Surface Water (SASW) and Subantarctic Mode Water (SAMW) are the lightest water masses that will be considered in this paper. Antarctic Intermediate Water (AAIW) and Antarctic Surface Water (AASW) will be treated as one water mass, denoted AAIW/AASW, based on the neutral density classifications given in Table 1. Piola and Gordon (1989) noted that most of the AAIW, with potential temperatures around 3.8°C and salinities less than 34.2, flowed through the gap that is denoted as the 54–54 Passage in this paper. Circumpolar Deep Water in the Scotia Sea can be divided into two types; Upper Circumpolar Deep Water (UCDW) and Lower Circumpolar Deep Water (LCDW). The presence of UCDW is usually associated with an oxygen minimum and a nutrient maximum, and also by a potential temperature maximum poleward of the PF. In addition, a variety of LCDW, Southeast Pacific Deep Water (SPDW), can be distinguished using silicate and neutral density values. The densest waters of the Pacific are higher in silicate than those of the Atlantic, which results in a residual signal that can be detected at Drake Passage and downstream in the ACC (Sievers and Nowlin, 1984; Peterson and Whitworth, 1989; Naveira Garabato et al., 2002). SPDW is characterised by high silicate values for waters with neutral density values greater than approximately 28.20.

Zenk (1981) and Wittstock and Zenk (1983) reported the results from a current meter deployed on the northern edge of Shag Rocks Passage in December 1979 and recovered in November 1980. Although Zenk (1981) and Wittstock and Zenk (1983) presented this current meter record, and although a few CTD stations have been occupied in the vicinity of the North Scotia Ridge (Gordon et al., 1977; Wittstock and Zenk, 1983), much remains unknown about the interaction of the ACC with the Ridge and the impact that this has on the structure of the current, deep water fluxes, and properties. This paper presents a detailed examination of the SAF and PF and their associated volume transports over the North Scotia Ridge, based on the first extensive hydrographic survey of the ridge. Estimates of eddy heat fluxes across the Polar Front from a current meter array deployed during this hydrographic survey have been presented by Walkden et al. (2008). Phytoplankton photophysiological variability and near surface nutrient chemistry, particularly results of iron bioavailability studies, from this same cruise were reported by Holeton et al. (2005).

2 The data set

Collection of the data set for the North Scotia Ridge Overflow Project (NSROP) was carried out during cruise JR80 of the *RRS James Clark Ross* between 23 April and 5 May 2003. Forty-nine full-depth CTD-LADCP (Conductivity-Temperature-Depth instrument, and Lowered Acoustic Doppler Current Profiler) stations were occupied along the ridge line of the North Scotia Ridge (Fig. 1). Stations were generally occupied whenever the bathymetry changed by more than 500 m, or every 40 km, if the bathymetry had not changed by 500 m within this distance. However, an exception to this was the shallow region between the station at 42.8°W and the station at 40.4°W, where due to time constraints, the separation was approximately 170 km (Fig. 1). Stations were deliberately spaced more closely when crossing fronts, and the average spacing of stations along the whole of the North Scotia Ridge was 23 km.

The CTD deployed on the cruise was a Sea-Bird Electronics SBE 911-plus instrument, with dual conductivity and temperature sensors. A 24-bottle rosette multisampler was used to obtain water samples for onboard calibration of salinity and for nutrient analysis. Salinity analyses were conducted on a Guildline Autosal 8400B salinometer, using P-series standard sea water as the reference standard. Water samples from the bottles were analysed for salinity, oxygen, silicate, and nitrate. The reported accuracies were 0.001°C in temperature, and 0.002 in salinity. Salinities quoted are calculated on the Practical Salinity Scale 1978 (Unesco, 1981), and are therefore given without units. Precision of the nutrient analyses were estimated to be 0.44 μmol kg^{-1} for nitrate, 0.99 μmol kg^{-1} for silicate, and 3.67 μmol kg^{-1} for oxygen. Holeton et al. (2005) presented results of phosphate and total dissolvable iron measurements from the JR80 cruise, and discussed the implications for phytoplankton communities.

The CTD frame also housed two RDI LADCPs, one a 150 kHz instrument and the other a 300 kHz instrument. Both LADCPs were broadband instruments and measurements were processed using University of Hawaii software. These instruments were mounted on the rosette frame, and both were downward-looking. The 150 kHz instrument was not operational for the first ten attempted stations, nor at the fifteenth and sixteenth stations. The data from the 300 kHz instrument were of good quality for the first fifteen stations, after which data quality deteriorated. Where available, the 150 kHz LADCP data were consistently better than the 300 kHz LADCP data. A ship-mounted 150 kHz ADCP was used to measure upper ocean currents, with an Ashtech ADU-2 GPS used to correct the data for errors in the heading of the ship's gyrocompass. Bottom track data were used to calibrate the ADCP for velocity scaling and misalignment errors.

3 Results

3.1 The frontal structure of the ACC over the North Scotia Ridge

Cruise JR80 consisted of two sections; an east-bound outward leg from the Falkland Islands to South Georgia, and a west-bound return leg from South Georgia to the Falkland Islands. A complete description of the ship movements during JR80, including Western Core Box stations, can be found in Holeton et al. (2005). In Fig. 2, high velocity flows coincident with changes in surface temperature can be seen in two locations, approximately 54.0°S, 55.5°W and 53.5°S, 48.0°W. These are the surface locations of the SAF and PF respectively, at this time. CTD casts were not occupied east of 50°W during the east-bound leg of the cruise due to adverse weather conditions, with the eastern CTD stations occupied on the return leg of the voyage (Fig. 1). During the intervening 11 days, the PF surface location was found to have moved approximately 1° (65 km) to the west. The PF appears to be constrained to flow within Shag Rocks Passage, which is approximately 180 km wide. An anticyclonic eddy-like feature can be seen at approximately 47°W (Fig. 2), lying over the approximately 980 m deep crest of the North Scotia Ridge on the eastern side of Shag Rocks Passage. This feature was also present at the same location in the west-bound ADCP data, and is most likely caused by interaction of the PF with the crest of the ridge at approximately 47°W. Shag Rocks Passage lies between 49.6°W and 47.1°W. The bathymetry of Shag Rocks Passage is shown in the section plots for potential temperature, salinity, neutral density, silicate, oxygen, nitrate in Figs. 3, 4, 5, 6, 7, and 8. The structure of this passage can be seen to consist of three main sills, with the western and eastern sill lying at approximately 3080 m, and the central sill at approximately 2870 m. A two-dimensional spatial interpolation was used to generate nitrate and silicate values between bottle measurements. Due to a technical malfunction, CTDO oxygen sensor measurements were not obtained, and therefore Fig. 7 presents oxygen bottle data only. There is general rising of isolines from west to east characteristic of the rising of isolines to south in conventional sections across the ACC.

Steep isoline slopes at approximately 55.5°W and 49.0°W indicate the presence of the SAF and PF, respectively (Figs. 3, 4, 5, 6, 7, 8). As noted by Gordon et al. (1977), voids in θ–S space can be used to detect the SAF and PF (Fig. 9(a)). The northernmost limit of the subsurface temperature minimum (<2°C) shallower than 200 m (Peterson and Whitworth, 1989) is also commonly used to identify the PF. All three indicators provide a consistent location for the PF. The crossing of the 200 m depth level by the 4°C isotherm is a widely used criterion for identifiying the SAF (Peterson and Whitworth, 1989). However this places the SAF poleward of the location given by frontal

jet, steep isolines and voids in θ–S space and hence we use the latter. It can be seen in 9(b) and 9(c) that the deepest waters for the stations along the North Scotia Ridge (black dots) have neutral density values that are less than those measured by Naveira Garabato et al. (2002) for ALBATROSS stations across Drake Passage and the Falkland Plateau/Georgia Basin section (grey dots in Fig. 9(b) and Fig. 9(c), respectively).

Geostrophic shears relative to the deepest common level were calculated from the temperature and salinity fields for each pair of adjacent stations along the North Scotia Ridge. These were then referenced to the mean of the LADCP velocity profiles for each station pair over a depth range of 200 m to the deepest common level. Offsets were calculated using the 150 kHz and 300 kHz LADCPs. These offsets were applied from the 150 kHz LADCP results where available, and from the 300 kHz LADCP for the other ten station pairs. Preference was given to the better quality 150 kHz data where available (Fig. 10). In most cases, the LADCP velocity shear profiles were consistent with the geostrophic shear. Both the SAF and the PF exhibit flows of 0.1–0.2 m s^{-1} close to the sea bed, including at depths of approximately 3000 m (Fig. 11). The flows associated with these fronts are therefore significant below 1000 m depth, in contrast with the assumption of Shaw et al. (2004). For six of the station pairs, better agreement with geostrophic shear was obtained using the ship-mounted ADCP measurements, averaged over depths of 46 m to 150 m, rather than the LADCP measurements. None of these six station pairs were in Shag Rocks Passage, and all had a deepest common level of less than 550 m. The resulting absolute geostrophic velocity for all station pairs is shown in Fig. 12.

The transmissometer data from along the North Scotia Ridge on the NSROP cruise gave no indication of murky bottom water, but this is likely to be due to an absence of sediment in Shag Rocks Passage rather than an indication of low flow velocities. Hollister and Elder (1969) reported murky bottom water along the North Scotia Ridge from a series of photographs of the seabed, and this was cited by Zenk (1981) as evidence in support of strong contour currents in the bottom of Shag Rocks Passage, as suggested by Gordon (1966).

Error estimates in the total and frontal volume transports were calculated using a Monte Carlo method assuming 3 cm s^{-1} as the standard deviation of a normal distribution of random perturbations to the barotropic flow. These perturbations were applied to individual velocity profiles 1000 times, and the root-mean-square deviation of the resulting transport calculated, following Naveira Garabato et al. (2003). An error estimate for the total transport was calculated by applying the perturbations across all station pairs. Error estimates for the fronts and inter-frontal zones were calculated by applying the perturbations across the relevant station pairs, which took into account the differing cross-sectional area of the water for differing station pair combina-

tions. It was assumed that the errors in the barotropic velocities at individual stations were uncorrelated with the errors in the barotropic velocities at adjacent stations.

Geostrophic transports were accumulated eastwards from Burdwood Bank along the North Scotia Ridge (Fig. 13). Bottom triangles were included by extrapolation of the deepest common level velocities to the seabed. The results are shown in Table 2, along with the upstream results for Drake Passage and the downstream results for the Falkland Plateau/Georgia Basin from Naveira Garabato et al. (2003). The total net transport was 117 ±10 Sv, with the baroclinic component relative to the deepest common level being 44 Sv. Across the North Scotia Ridge, the transport associated with the SAF was 52 ±4 Sv and the transport associated with the PF was 58 ±5 Sv. The PFZ contributes a net transport of 8 ±4 Sv, to give a combined net transport for the PF and PFZ of 66 ±6 Sv. For the region east of the PF, the transport across the North Scotia Ridge is not significant.

The SAF and the PF lie on the western side of the 54–54 Passage and Shag Rocks Passage, respectively, where the topography slopes downwards towards the east. ADCP measurements indicate that the PF, or at least the surface expression of the PF, lay on the eastern side of Shag Rocks Passage on the outward leg of the journey. This movement within the Passage has been noted by previous authors, for example by Mackintosh (1946).

3.2 The water mass structure of the ACC over the North Scotia Ridge

The total net LADCP referenced transports across the North Scotia Ridge associated with each water mass are shown in Fig. 14 and listed in Table 3. The transports associated with the Subantarctic Front (SAF) and Polar Front (PF) for each water mass are also presented in Table 3.

In the PFZ, the density class associated with AAIW/AASW is observed between approximately 150 dbar and 700 dbar. The transport associated with this density class was found to be 37 Sv. The AAIW/AASW-UCDW boundary along the western side of the ridge has potential temperatures approaching 2.7 °C.

Along the North Scotia Ridge, a band of oxygen values less than 200 μmol kg^{-1} coincident with the UCDW-LCDW boundary in Shag Rocks Passage was observed, with minima approaching 170 μmol kg^{-1} (Fig. 7). Nitrate values greater than 32 μmol kg^{-1} lie within the UCDW water mass layer (Fig. 8). The local minima of nitrate lies within the LCDW layer. The 1.8 °C isotherm lies on the UCDW-LCDW boundary. In Drake Passage, LCDW/SPDW can be found spanning the width of the passage (Naveira Garabato et al., 2003).

In contrast, at the North Scotia Ridge, LCDW/SPDW is present only in Shag Rocks Passage and further eastwards (Fig. 5). None of the LCDW/SPDW is associated with the SAF at the North Scotia Ridge. Naveira Garabato et al. (2003) showed (Fig. 4 of that paper) that LCDW/SPDW then spills over the Falkland Plateau, but does not reach the region where the SAF was observed. A maximum silicate value of approximately 124 μmol kg^{-1} was observed in the deepest waters of Shag Rocks Passage (Fig. 6). The implications for the presence of SPDW will be discussed further below. It can be seen in Fig. 3 that the waters to the west of Shag Rocks Passage are warmer than 2°C at all depths. Waters with potential temperatures below 2°C in Shag Rocks Passage are predominantly LCDW/SPDW, with neutral densities less than 28.00 kg m^{-3}. The highest salinity water, with salinities up to 34.763, lies in the LCDW core in Shag Rocks Passage. The PF lay to the east of the deepest station (3151 dbar). Potential temperatures at comparable depths were therefore much colder on the eastern sill, at 0.27°C, than on the western sill, at 0.58°C. Waters with potential temperatures below 2°C were observed at pressures of approximately 100 dbar to 430 dbar, in two distinct patches to the east of the PF. Water east of Shag Rocks Passage, with a potential temperature minimum of 0.29°C and salinity approximately 34 (Fig. 9(a)), is characteristic of Winter Water, the remnant of the previous winter's mixed layer which has become capped by fresh water and warmed at the surface by insolation.

No waters matching the density of WSDW were found along the North Scotia Ridge (Fig. 9(b)). The possibility of WSDW traversing the North Scotia Ridge is considered in section 4.1.2.

4 Discussion

4.1 Exchange of water between the SAF and PF

In Fig. 9(a) intrusions can be seen across each front for the neutral density class between 27.18 and 27.55. Gordon et al. (1977) observed similar intrusions for data collected in the vicinity of the North Scotia Ridge. Such intrusions are direct evidence of the cross-frontal exchange of water masses. Such exchanges may be caused by the interaction of fronts with bathymetric features. To gain further insight on the interaction of the fronts with bathymetry, in Fig. 15 we present Eddy Kinetic Energy (EKE) calculated from the AVISO joint TOPEX/ERS sea level anomaly product, covering the period 1992 to 2005, after Ducet et al. (2000). The region of highest EKE indicates the influence of eddy activity associated with the SAF and PF, and follows the southern flank of the North Scotia Ridge, as far as Shag Rocks Passage in the case of the PF. The decrease in EKE on the northern side of the ridge is due

to the influence of the ridge system reducing eddy activity. It can be observed that the North Scotia Ridge plays a major role in dictating the pattern of EKE, with values south of the ridge being at least a factor of two higher than those north, and small "plumes" of elevated EKE seeming to leak across the ridge in the vicinity of the gaps, e.g. Shag Rocks Passage. A detailed consideration of the North Scotia Ridge's role in eddy/topographic interaction is beyond the scope of this paper. A region of elevated topography is present at approximately 56°S, 55°W. This topographic feature, lying upstream of the North Scotia Ridge, may play a crucial role in the transfer of water between the fronts. The feature is approximately 100 km in diameter and rises from 3500 m depth at its base to 2000 m at the summit in the topographical database of Smith and Sandwell (1997). The paths of the SAF and PF converge there along a path of converging f/H contours, where f is the Coriolis parameter, and H is the water depth. The path of the SAF is constrained on the west by the steep topography of the North Scotia Ridge, and the gap between the ridge and the 3000 m contour at the base is approximately 88 km wide. In Moore et al. (1997, Plate 4), one can see another smaller region of elevated topography to the south-east that lies in the f/H coutour path of the PF. The gap between these two regions that the mean path of the PF passes through is less than 80 km wide. It seems likely that this region is the main location at which transfers of water between the SAF and PF occur. The height of the topography is 2000 m, which corresponds to the depth at which LCDW is found in the PF at the North Scotia Ridge, and at the PF in Drake Passage (Naveira Garabato et al., 2003)

SSH anomalies spanning the time period of the cruise are shown in Fig. 16. The presence of a sequence of cyclonic/anticyclonic eddies south of the North Scotia Ridge can be seen, especially the western part of the ridge. Along the cruise track, the main notable event is the formation of a cyclonic eddy close to Shag Rocks Passage some time around 29 April 2003, and its propagation through the passage during the first half of May. This would give cyclonic anomalies in the velocity field around Shag Rocks Passage during this time (i.e. stronger-than-average northward velocities on the western side of the passage, and the converse on the eastern side). Before this time, surface velocities along the cruise track are not very different from their long-term mean values, including at Shag Rocks Passage.

Naveira Garabato et al. (2003) reported the transports associated with the SAF and the PF for Drake Passage to be 31 $\pm$7 Sv and 80 $\pm$7 Sv, respectively. Because of current reversals, the total net transport of the SAF and PF combined is only approximately 94 Sv in Drake Passage. Inclusion of flows between the PF and the SACCF yields a net transport of 121 Sv, which is closer to the total transport for the SAF and PF across the North Scotia Ridge reported here. This suggests that the transport of the SAF and PF across the North Scotia Ridge incorporates waters not associated with those

two fronts at Drake Passage. Although the Drake Passage and North Scotia Ridge measurements were taken four years apart, the similar values for total net transport associated with these two fronts allows the inference to be made that a transfer of water from the PF to the SAF upstream of the North Scotia Ridge occurs. This inference is made due to the apparent increase in the transport associated with the SAF at the North Scotia Ridge compared with Drake Passage, and decrease in the transport associated with the PF at the North Scotia Ridge compared with Drake Passage. Further investigations into the exact nature and mechanism of this inferred transfer are needed using numerical modelling or perhaps observing the spread of a tracer. Since in our non-contemporaneous measurements at Drake Passage and the North Scotia Ridge, it is possible that there is some aliasing of interannual variability, ideally one would want simultaneous sections up and downstream.

Through the use of a box inverse model, Naveira Garabato et al. (2003) calculated the total net transport of AAIW/AASW at Drake Passage to be approximately 35 Sv, with 31 % of this transport associated with the SAF and 66 % associated with the PF. At the North Scotia Ridge, the total net transport was found to be very close to that reported by Naveira Garabato et al. (2003) at Drake Passage, at 37 Sv. However, in contrast to Drake Passage, approximately 60 % of the transport of AAIW/AASW across the North Scotia Ridge was associated with the SAF and only 30 % with the PF. This division of AAIW/AASW transport more closely resembles that reported by Naveira Garabato et al. (2003) for the Falkland Plateau/Georgia Basin region, where 66 % of AAIW/AASW transport was associated with the SAF. This suggests a transfer of approximately 10 Sv of AAIW/AASW from the PF to the SAF. There is also a compensating transfer of lower UCDW and LCDW from the SAF to the PF. It can be seen in Fig. 12 that the reduction in AAIW/AASW transport associated with the PF across the North Scotia Ridge is a consequence of the restricted vertical extent of the water mass at that front. The transfer of the deepest UCDW and LCDW water masses from the SAF to the PF occurs due to the SAF flowing over the North Scotia Ridge at depths shallower than these water masses reside. This transfer of transports between the PF and the SAF was inferred by Naveira Garabato et al. (2003) to be part of a cross-ACC overturning circulation. Naveira Garabato et al. (2003) speculated this overturning was driven by interaction with the North Scotia Ridge. From the observations along the North Scotia Ridge outlined above, one can conclude that this transfer takes place at or upstream of the North Scotia Ridge.

4.2 Do NADW and WSDW flow through Shag Rocks Passage?

NADW was detected by Naveira Garabato et al. (2002) in the region immediately adjacent to the Maurice Ewing Bank, (Fig. 9(c)), and it was inferred that NADW was entrained across the Falkland Plateau from the north. There is no evidence of this NADW signal reaching the North Scotia Ridge (Fig. 9(a)).

Naveira Garabato et al. (2002) reported that WSDW was not present in the PF at Drake Passage, although it was found poleward of the SACCF. In the deeper Georgia Basin north-east of the North Scotia Ridge, Naveira Garabato et al. (2002) found evidence for WSDW (grey points in Figure 4 of that paper), but it appears that WSDW does not pass through Shag Rocks Passage, or may do so only intermittently.

The waters at the North Scotia Ridge are fresher and colder along isopycnals than at Drake Passage (Fig. 9(b)). This is due to mixing processes in the Scotia Sea, where the warmer and saltier waters of Pacific origin observed at Drake Passage interact with waters entering from the Weddell Sea.

The density of WSDW is such that it would lie below the sills of Shag Rocks Passage, if it were present on the south side of the ridge. However, WSDW has been observed in the Malvinas Chasm, to the north of the North Scotia Ridge (Locarnini et al., 1993). This is likely to be water that has flowed around the eastern side of South Georgia. It is very unlikely to have traversed the North Scotia Ridge. Episodic high-speed bursts of cold water were reported by Zenk (1981) from current meter observations, with 15 % of the all daily observations recording water with in situ temperatures less than 0.6°C and speeds greater than 28 cm s^{-1}. The current meter records described by Zenk (1981) were 35 m and 85 m above the sea floor in waters 3008 m deep, but no salinity measurements were made. The minimum in situ temperature recorded by Zenk (1981) was 0.1°C. The lowest in situ temperature observed in the deep waters of Shag Rocks Passage during the NSROP cruise was 0.45°C, which is within the range of the current meter results of Zenk (1981). The episodic bursts were taken by Zenk (1981) to indicate overflows through SRP of water formed by mixing of waters from the Weddell Sea and the eastern Pacific. Wittstock and Zenk (1983), analysing the same data set, concluded that the water observed was Antarctic Bottom Water. However, Locarnini et al. (1993) disagreed with this conclusion, and suggested that WSDW found in the Malvinas Chasm to the north of Shag Rocks Passage originated as westward-flowing water from the Georgia Basin. This conclusion was based on reanalysis of the results of Wittstock and Zenk (1983) as well as other data sets. However, Whitworth et al. (1991) inferred from flows of CDW that a branch of the ACC goes through Shag Rocks Passage and then eastwards along the Malvinas Chasm. An eastward-travelling

branch of the PF was also reported by Naveira Garabato et al. (2002). We found no evidence for the overflow of WSDW through Shag Rocks Passage, and LADCP data indicated that flow of the PF through the western side of the passage was northwards at all depths. It is possible that WSDW enters the Malvinas Chasm on the southern side, flowing westwards, and then returns eastwards, with some of the WSDW mixing upwards into the LCDW layer within the PF. There is evidence from the deployment of Argo floats that supports our suggestion above that the flow follows f/H contours around the bathymetry of the Malvinas Chasm in a clockwise fashion, for example http://www.pac.dfo-mpo.gc.ca/sci/osap/projects/argo/movies/Drake.avi (last accessed 28 September 2009). Although the mean flow is unlikely to follow a clockwise path all the way up the Chasm and back, the flow is in general clockwise and more constrained at the western end, with occasional episodes extending further. This could account for the net inflow of 0.5 Sv of WSDW into the Scotia Sea at the Georgia Basin boundary noted by Naveira Garabato et al. (2003).

4.3 Baroclinic versus barotropic transports

The total net LADCP referenced transport through Drake Passage in 1999 was 148 ± 14 Sv (Naveira Garabato et al., 2003), with a baroclinic transport relative to the deepest common level of 137 Sv. The ratio of the baroclinic transport to the barotropic transport was also high in the year 2000 at the SR1b WOCE section, east of Drake Passage and upstream of the North Scotia Ridge (Cunningham et al., 2003). Naveira Garabato et al. (2003) calculated the total net LADCP referenced transport across the Falkland Plateau and through the Georgia Basin in 1999 to be 119 ± 12 Sv, with a baroclinic transport relative to the deepest common level of 56 Sv. As stated in section 3.1, for the North Scotia Ridge the total net transport was 117 ±10 Sv, with a baroclinic component relative to the deepest common level of 44 Sv. There is therefore an apparent switch from predominantly baroclinic transport at Drake Passage to transport with a larger barotropic component along the Falkland Plateau/Georgia Basin section and at the North Scotia Ridge. This is largely due to the difference in topography between Drake Passage and the North Scotia Ridge.

4.4 Large-scale implications of the ACC interaction with the North Scotia Ridge

The total net transport across the North Scotia Ridge was found to be 117 ±10 Sv. This is in agreement with the transport for waters overflowing the North Scotia

Ridge predicted by Naveira Garabato et al. (2003), 119 ±12 Sv, and therefore these measurements support the assumptions made in that paper.

The transport across the North Scotia Ridge east of the PF is not significant. Arhan et al. (2002) inferred a northward transport of 14±11 Sv over the North Scotia Ridge east of the PF. At 54°S, 40°W there is an approximately 2000 m deep gap that will be referred to in this paper as Black Rock Passage. A reversal in flow direction through the Black Rock Passage can be seen in Fig. 2. This might be linked to periodic surges of water along the Malvinas Chasm, such as those suggested by Locarnini et al. (1993), but is more likely to be attributable to temporal variability and/or the eddy field. Although the flow through the Black Rock Passage makes no overall contribution to the total net transport across the NSR, it is a potential site for deep water exchange between the Scotia Sea and the area to the north-west of South Georgia. Data from the ship-mounted ADCP indicate that the flow through the Black Rock Passage was southwards on the outward cruise leg, but northward on the return leg (Fig. 2), but it is likely that the ADCP measurements include inertial variations due to the action of wind on the mixed layer. It was on the return leg that CTD-LADCP stations were occupied and full depth measurements of transport made. The difference between the transport observed by Arhan et al. (2002) and the NSROP could be due to variability in the division of transports between the fronts due to interaction with topography.

4.5 Does SPDW flow through Shag Rocks Passage?

The maximum silicate value observed in Shag Rocks Passage, 124 μmol kg^{-1}, is lower than those identified as the remnants of SPDW by Peterson and Whitworth (1989) and Arhan et al. (1999) in the Falkland Escarpment, downstream of the North Scotia Ridge and Falkland Plateau. It is also lower than the concentrations of 135 μmol kg^{-1} and 125 μmol kg^{-1} at Drake Passage and Georgia Basin respectively (Naveira Garabato et al., 2002). At best a highly eroded silicate signal of SPDW might be identified in Shag Rocks Passage, and also at the approximately 2000 m deep Black Rock Passage (Fig. 6). Peterson and Whitworth (1989) and Naveira Garabato et al. (2002) indicated that the overflow of SPDW through Shag Rocks Passage may be intermittent. If the measurements for the NSROP were made at a time when this overflow did not occur, or was weak, this may account for the lower values observed here. However, another possibility is that none of the SPDW reported in the Georgia Basin by Naveira Garabato et al. (2002) had overflowed the North Scotia Ridge; they suggested that the SPDW observed in the Georgia Basin may have been transported by the flow associated with the SACCF. Similarly, the Black Rock Passage is a possible pathway for the exchange of deep water across the North Scotia Ridge, but the NSROP measurements indicate that

any such transfer is intermittent.

4.6 Does a branching of the PF occur in Shag Rocks Passage?

The total net LADCP-referenced transport for the ALBATROSS section across the Falkland Plateau and the Georgia Basin was 129 ± 21 Sv (Arhan et al., 2002). The baroclinic transport relative to the bottom was 56 Sv. Arhan et al. (2002) gave the transport associated with the SAF as 52 ± 6 Sv, while the transport associated with the PF had two branches, with a net transport of 68 ± 10 Sv. For the NSROP, the transport associated with the PF is found to be 58 ± 5 Sv, which, although at the lower end of the scale, is within the range estimated by Arhan et al. (2002).

Arhan et al. (2002) reported a high velocity core in the western branch of the PF in the UCDW, at approximately 1700 m depth in the LADCP measurements. This feature was apparently transitory in nature, as it was not observed in the geostrophic field. No such feature was observed along the North Scotia Ridge, which lends weight to the suggestion of Arhan et al. (2002) that the branching of the PF observed by those authors was topographically induced and occurred downstream of the North Scotia Ridge. In Fig. 11, three high velocity cores of the PF, each corresponding to one of the three sills of Shag Rocks Passage can be seen. This illustrates the bottom-reaching nature of the front and the link between frontal structure and sea bed topography. However, it does not necessarily precondition the PF to undergo the splitting observed by Arhan et al. (2002).

Acknowledgements

The North Scotia Ridge Overflow Project was funded by the Natural Environment Research Council grant NER/G/S/2001/00006 through the Antarctic Funding Initiative. We wish to thank the officers and crew of cruise JR80 of the *RRS James Clark Ross* for all their efforts in collecting this data set. Our thanks go to Louise Sime, Glen Richardson, Manfredi Manizza, Louise Brown, and Claire Holeton for assistance in collecting and processing data, and to Ian Waddington, John Wynar, and Steve Mack for technical assistance. We particularly want to thank Alberto Naveira Garabato for his extensive help and advice in the preparation of this paper. Thanks also to the three anonymous reviewers for their very helpful and constructive comments.

References

Arhan, M., Heywood, K. J., and King, B. A., 1999. The deep waters from the Southern Ocean at the entry to the Argentine Basin. Deep-Sea Research II 46, 475–499.

Arhan, M., Naveira Garabato, A. C., Heywood, K. J., and Stevens, D. P., 2002. The Antarctic Circumpolar Current between the Falkland Islands and South Georgia. Journal of Physical Oceanography 32, 1914–1931.

Cunningham, S. A., Alderson, S. G., King, B. A., and Brandon, M. A., 2003. Transport variability of the Antarctic Circumpolar Current in Drake Passage. Journal of Geophysical Research 108(C5), 8084, doi:10.1029/2001JC001147.

Deacon, G. E. R., 1933. A general account of the hydrology of the South Atlantic Ocean. Discovery Reports, 7, 171–238.

Ducet, N., Le Traon, P.-Y., and Reverdin, G. (2000). Global high resolution mapping of ocean circulation from TOPEX/Poseidon and ERS-1/2. Journal of Geophysical Research, 105, 19477–19498.

García, M. A., Bladé, I, Cruzado, A., Velásquez, Z., García, H., Puigdefàbregas, J. and Sospedra, J., 2002. Observed varibility of water properties and transports on the World Ocean Circulation Experiment SR1b section across the Antarctic Circumpolar Current. Journal of Geophysical Research, 107(C10),3162, doi:10.1029/2000JC00027 7.

Gordon, A. L., 1966. Potential temperature, oxygen and circulation of bottom water in the Southern Ocean. Deep Sea Research 13, 1125–1138.

Gordon, A. L., Georgi, D. T., and Taylor, H. W., 1977. Antarctic Polar Frontal Zone in the western Scotia Sea - Summer 1975. Journal of Physical Oceanography, 7, 309–328.

Herdman, H. F. P., 1932. Report on soundings taken during the Discovery Investigations. Discovery Reports 6, 205–236.

Holeton, C. L., Nédélec, F., Sanders, R., Brown, L., Moore, C. M., Stevens, D. P., Heywood, K. J., Statham, P. J. and Lucas, C. H., 2005. Physiological state of phytoplankton communities in the Southwest Atlantic sector of the Southern Ocean, as measured by fast repetition rate fluorometry. Polar Biology 29, 44–52, doi 10.1007/s00300-005-0028-y.

Hollister, C. D. and Elder, R. B., 1969. Contour currents in the Weddell Sea. Deep-Sea Research 16, 99–101.

Jackett, D. and McDougall, T. J., 1997. A neutral density variable for the world's oceans. Journal of Physical Oceanography 27, 237–263.

Locarnini, R. A., Whitworth III, T., and Nowlin Jr., W. D., 1993. The importance of the Scotia Sea on the outflow of Weddell Sea Deep Water. Journal of Marine Research 51, 135–153.

Mackintosh, N. A., 1946. The Antarctic Convergence and the distribution of surface temperatures in Antarctic waters. Discovery Reports, 23, 177–212.

Moore, J. K., Abbott, M. R., and Richman, J. G., 1997. Variability in the location of the Antarctic Polar Front (90^o–20^o W) from satellite sea sur-

face temperature data. Journal of Geophysical Research, 102(C13), 27825–27833.

Naveira Garabato, A. C., Heywood, K. J., and Stevens, D. P., 2002. Modification and pathways of Southern Ocean deep waters in the Scotia Sea. Deep-Sea Research I 49, 681–705.

Naveira Garabato, A. C., Stevens, D. P., and Heywood, K. J., 2003. Water mass conversion, fluxes, and mixing in the Scotia Sea diagnosed by an inverse model. Journal of Physical Oceanography 33, 2565–2587.

Orsi, A. H., Whitworth III, T., and Nowlin Jr., W. D., 1995. On the meridional extent and fronts of the Antarctic Circumpolar Current. Deep-Sea Research 42, 641–673.

Peterson, R. G. and Whitworth III, T., 1989. The Subantarctic and Polar Fronts in relation to deep water masses through the Southwestern Atlantic. Journal of Geophysical Research 94(C8), 10817–10838.

Piola, A. and Gordon, A. L. 1989. Intermediate water in the southwestern South Atlantic. Deep-Sea Research 36, 1–16.

Reid, J. L., Nowlin, Jr., W. D., and Patzert, W. C., 1977. On the characteristics and circulation of the Southwestern Atlantic Ocean. Journal of Physical Oceanography, (7), 62–91.

Shaw, P. W., Arkhipkin, A. I., and Al-Khairulla, H., 2004. Genetic structuring of Patagonian toothfish populations in the Southwest Atlantic Ocean: the effect of the Antarctic Polar Front and deep-water troughs as barriers to genetic exchange. Molecular Ecology 13, 3293–3303.

Sievers, H. A. and Nowlin Jr., W. D., 1984. The stratification and water masses at Drake Passage. Journal of Geophysical Research 89, 10489–10514.

Smith, W. H. F. and Sandwell, D. T., 1997. Global sea floor topography from satellite altimetry and ship depth soundings. Science 277, 1956–1962.

Sun, C., and Watts, D. R., 2001. A circumpolar gravest empirical mode for the Southern Ocean hydrography. Journal of Geophysical Research 106(C2), 2833–2855.

Thorpe, S. E., Heywood, K. J., Stevens, D. P., and Brandon, M. A., 2004. Tracking passive drifters in a high resolution ocean model: Implications for interannual variability of larval krill transport to South Georgia. Deep-Sea Research I 51, 909–920.

Unesco, 1981. The Practical Salinity Scale 1978 and the International Equation of State of Seawater 1980. Tenth report of the joint panel on oceanographic tables and standards, Unesco, Paris, France, 13–17. Unesco Technical Papers in Marine Science, No. 36

Walkden, G. J., Heywood, K. J., and Stevens, D. P., 2008. Eddy heat fluxes from direct current measurements of the Antarctic Polar Front in Shag Rocks Passage. Geophysical Research Letters 35, L06602, doi:10.1029/2007GL032767.

Whitworth III, T., 1983. Monitoring the transport of the Antarctic Circumpolar Current at Drake Passage. Journal of Physical Oceanography 13, 2045–2057.

Whitworth III, T. and Peterson, R. G. 1985. Volume transport of the Antarctic Circumpolar Current from bottom pressure measurements. Journal of Physical Oceanography 15, 810–816.

Whitworth III, T., Nowlin Jr., W. D., Pillsbury, R. D., Moore, M. I., and Weiss, R. F., 1991. Observations of the Antarctic Circumpolar Current and deep boundary current in the southwest Atlantic. Journal of Geophysical Research 96, 15105–15118.

Wittstock, R.-R. and Zenk, W., 1983. Some current observations and surface T/S distribution from the Scotia Sea and the Bransfield Strait during early austral summer 1980/81. Meteor Forschungs-Ergenbnisse, Riehe A/B 24, 77–86.

Zenk, W., 1981. Detection of overflow events in the Shag Rocks Passage, Scotia Ridge. Science 213, 1113–1114.

Table 1

Definitions of water masses in the Scotia Sea. Taken from Naveira Garabato et al. (2002) , based on Reid et al. (1977), Sievers and Nowlin (1984), and Arhan et al. (1999)

Water mass	**Abbreviation**	**Neutral density**
Subantarctic Surface Water	SASW	$\gamma^n < 26.90$
Subantarctic Mode Water	SAMW	$26.90 < \gamma^n < 27.18$
Antarctic Surface Water/	AASW/	$27.18 < \gamma^n < 27.55$
Antarctic Intermediate Water	AAIW	
Upper Circumpolar Deep Water	UCDW	$27.55 < \gamma^n < 28.00$
Lower Circumpolar Deep Water/	LCDW/	$28.00 < \gamma^n < 28.26$
Southeast Pacific Deep Water	SPDW	
Weddell Sea Deep Water	WSDW	$28.26 < \gamma^n < 28.40$

Table 2

Total net transports at Drake Passage, over the North Scotia Ridge, and across the Falkland Plateau/Georgia Basin. North Scotia Ridge results are from the work described in this paper, and compare favourably with the prediction of Naveira Garabato et al. (2003) of 119±12 as the total net transport over the ridge. Drake Passage and Falkland Plateau/Georgia Basin results are taken from Naveira Garabato et al. (2003), and were output from an inverse model. Transport not associated with either the Subantarctic Front (SAF) or the Polar Front (PF) is due to residual flow in the areas outside the frontal zones. Two branches of the PF exist over the Falkland Plateau/Georgia Basin.

Water mass	**Total Net Transport [Sv]**	**Transport associated with SAF [Sv]**	**Transport associated with PF [Sv]**
Drake Passage	143±13	31±7	80±7
North Scotia Ridge	117±10	52±4	58±5
Falkland Plateau/ Georgia Basin	119±12	48±4	37±6 and 52±6

Table 3

Transports over the North Scotia Ridge associated with the water masses listed in Table 1. Transport not associated with either the Subantarctic Front (SAF) or the Polar Front (PF) is due to residual flow in the areas outside the frontal zones.

Water mass	**Total Net Transport [Sv]**	**Transport associated with SAF [Sv]**	**Transport associated with PF [Sv]**
SASW	3	2	0
SAMW	13	8	5
AASW/AAIW	37	23	12
UCDW	45	18	27
LCDW/SPDW	20	0	19
WSDW	0	0	0

Figure captions

Fig. 1. The bathymetry of the North Scotia Ridge region derived from satelitte altimetry (Smith and Sandwell, 1997). CTD stations for the North Scotia Ridge Overflow Project are shown as diamonds. ALBATROSS stations across the Falkland Plateau and Georgia Basin and across Drake Passage are denoted by squares. Shag Rocks Passage is denoted by SRP. Shading is every 1000 m and isobaths are every 500 m. The historical mean frontal positions are indicated by black lines. The positions of SAF and SACCF are from Orsi et al. (1995) and the position of the PF is from Moore et al. (1997).

Fig. 2. Underway ADCP velocity vectors, averaged over 54–102 m, with 10 minute time bins smoothed with an hourly running mean. Velocity vectors are coloured by surface water temperature, which is between 2 °C and 9 °C, in 0.5 °C intervals. The thermosalinograph measured water temperatures from an intake at approximately 5 m depth. Velocity values are indicated by the length of the lines, with a standard 1 m s^{-1} line shown at the top right of the figure. The lower figure shows the outward track along the North Scotia Ridge, while the upper figure shows the corresponding return track along the ridge to Shag Rocks Passage. Once Shag Rocks Passage was crossed on the return leg of the cruise, the ship took a direct route to the Falkland Islands rather than following the ridge. For this reason, only data for half of the return leg is presented here.

Fig. 3. Potential temperature section for the North Scotia Ridge. Values colder than 2°C are shaded grey. Dark lines denote water mass boundaries in neutral density, with values as defined in Fig. 5. The location of the Polar Front (PF) and Subantarctic Front (SAF) are marked, with the Polar Frontal Zone (PFZ) and Antarctic Zone (AAZ) indicated. Station locations are shown along the lower axis.

Fig. 4. Salinity section for the North Scotia Ridge. Dark lines denote water mass boundaries in neutral density, with values as defined in Fig. 5. Values between 34.4 and 34.7 are shaded grey. The location of the Polar Front

(PF) and Subantarctic Front (SAF) are marked. Station locations are shown along the lower axis, with the Polar Frontal Zone (PFZ) and Antarctic Zone (AAZ) indicated.

Fig. 5. Neutral density section defining the boundaries of water masses. Water masses with γ^n values less than 27.18 are denoted SASW/SAMW, while those with γ^n values between 27.18 and 27.55 are denoted AAIW/AASW. UCDW denotes waters with γ^n values between 27.55 and 28.00, while LCDW denotes waters with γ^n greater than 28.00. The boundary is also marked for γ^n values greater than 28.20, which is the nominal boundary for SPDW.

Fig. 6. Silicate section for the North Scotia Ridge. Dark lines denote water mass boundaries in neutral density, with values as defined in Fig. 5. Values with silicate values greater than 120 μmol kg^{-1} are shaded grey. The location of the Polar Front (PF) and Subantarctic Front (SAF) are marked, with the Polar Frontal Zone (PFZ) and Antarctic Zone (AAZ) indicated. Dots indicate the location of bottles used to construct the section. Station locations are shown along the lower axis.

Fig. 7. Dissolved oxygen section for the North Scotia Ridge. Dark lines denote water mass boundaries in neutral density, with values as defined in Fig. 5. Values with oxygen values less than 200 μmol kg^{-1} are shaded grey. The location of the Polar Front (PF) and Subantarctic Front (SAF) are marked, with the Polar Frontal Zone (PFZ) and Antarctic Zone (AAZ) indicated. Dots indicate the location of bottles used to construct the section. Station locations are shown along the lower axis.

Fig. 8. Nitrate section for the North Scotia Ridge. Dark lines denote water mass boundaries in neutral density, with values as defined in Fig. 5. Values with nitrate values greater than 32 μmol kg^{-1} are shaded grey. The location of the Polar Front (PF) and Subantarctic Front (SAF) are marked, with the Polar Frontal Zone (PFZ) and Antarctic Zone (AAZ) indicated. Dots indicate the location of bottles used to construct the section. Station locations are shown along the lower axis.

Fig. 9. (a) Potential temperature versus salinity, for the 49 CTD stations occupied along the North Scotia Ridge (black dots). Voids in θ–S space

mark the SAF and PF. Lines of neutral density (black lines, water mass separations) (Jackett and McDougall, 1997) are as for Fig. 5. (b) Close-up of densest water classes for the North Scotia Ridge (black dots) and for Drake Passage (grey dots - ALBATROSS cruise data from Naveira Garabato et al. (2002); stations for the ALBATROSS cruise are shown in Fig. 1). (c) Close-up of the densest water classes for the North Scotia Ridge (black dots) and for the Falkland Plateau/Georgia Basin (grey dots - ALBATROSS cruise data from Naveira Garabato et al. (2002); stations for the ALBATROSS cruise are shown in Fig. 1).

Fig. 10. Geostrophic shear for the pair of stations located at 49.1 °W and 48.9 °W, in Shag Rocks Passage. The thin black line is the geostrophic profile derived from CTD data, before any adjustments. The thick black line is the geostrophic profile adjusted by a constant offset based on the average value of the LADCP data. 150 kHz LADCP data are shown as grey broken lines. The darkest grey line is the mean of the corresponding light grey dashed (eastern station) and medium grey dashed (western station) lines. The short black solid line is the ship-mounted ADCP data to 150 m depth.

Fig. 11. LADCP velocity in m s^{-1} for station pairs along the North Scotia Ridge. Dark lines denote water mass boundaries in neutral density, with values as defined in Fig. 5.

Fig. 12. Geostrophic velocity in m s^{-1} referenced to LADCP/ADCP profiles for station pairs along the North Scotia Ridge. Dark lines denote water mass boundaries in neutral density, with values as defined in Fig. 5.

Fig. 13. Cumulative volume transports for NSROP. The solid line indicates the total net transport, obtained by referencing to LADCP/ADCP, while the dashed line denotes the baroclinic transport referenced to the deepest common level. Error bars for the total net transport were calculated from a Monte Carlo analysis and are shown as grey shading.

Fig. 14. Cumulative volume transports, accumulated from west to east, for water masses SASW, SAMW, AAIW/AASW, UCDW, and LCDW for the North Scotia Ridge.

Fig. 15. Eddy Kinetic Energy (EKE) calculated from the AVISO joint TOPEX/ERS sea level anomaly product, covering the period 1992 to 2005. Units are cm^2s^{-2}.

Fig. 16. Sequence of Sea Surface Height (SSH) anomalies spanning the time period of the cruise, specifically 22 April to 13 May 2003. Units are cm. Note in particular the negative SSH anomaly in the vicinity of Shag Rocks Passage during May 6-13, indicative of a cold-core (cyclonic) eddy present here at this time.

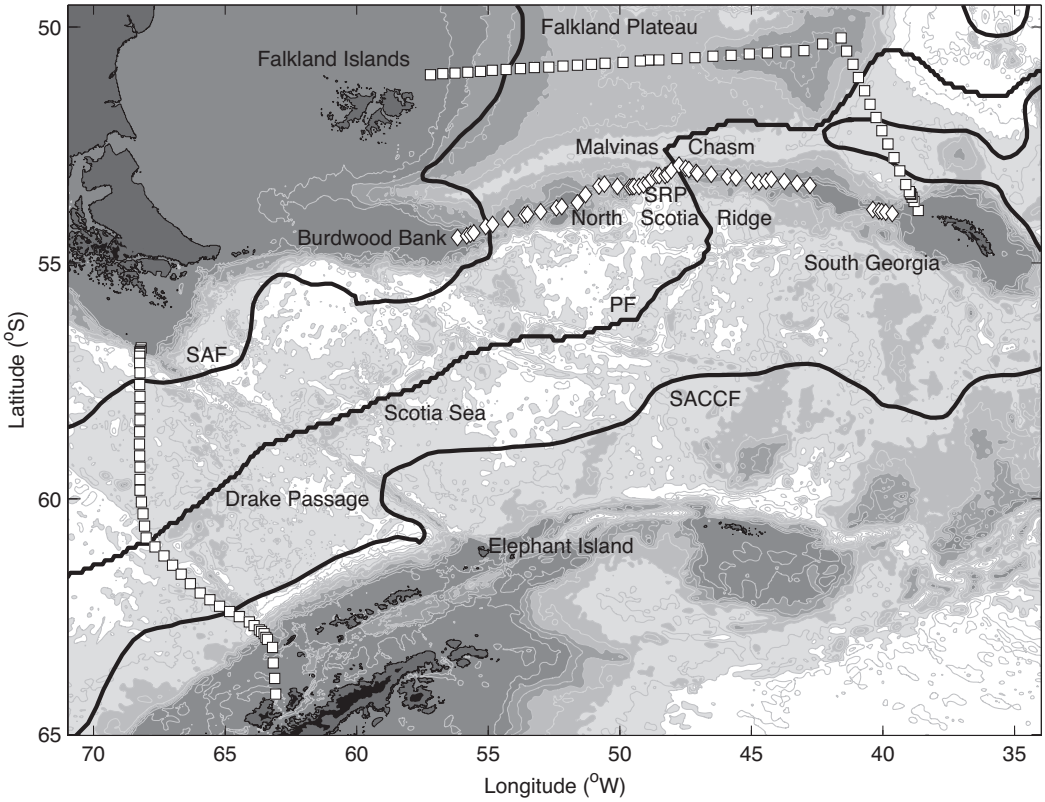

Fig. 1. The bathymetry of the North Scotia Ridge region derived from satelitte altimetry (Smith and Sandwell, 1997). CTD stations for the North Scotia Ridge Overflow Project are shown as diamonds. ALBATROSS stations across the Falkland Plateau and Georgia Basin and across Drake Passage are denoted by squares. Shag Rocks Passage is denoted by SRP. Shading is every 1000 m and isobaths are every 500 m. The historical mean frontal positions are indicated by black lines. The positions of SAF and SACCF are from Orsi et al. (1995) and the position of the PF is from Moore et al. (1997).

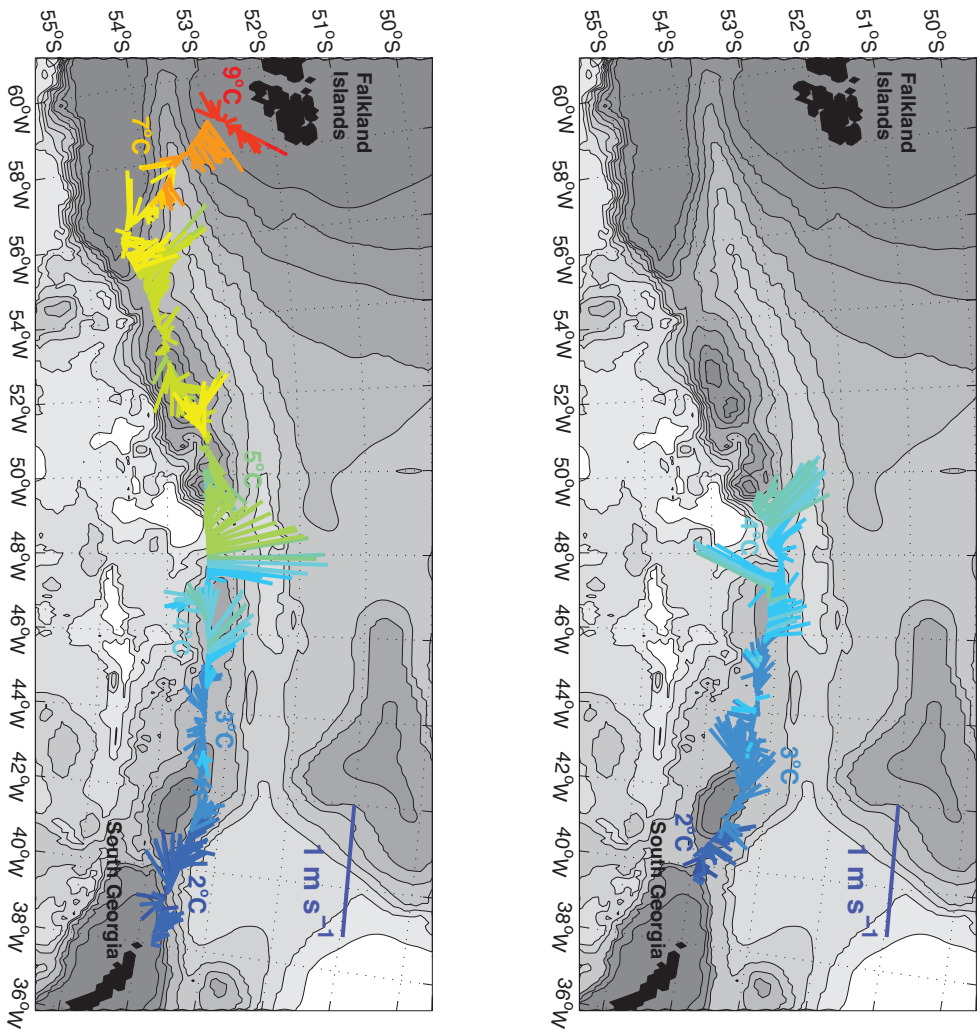

Fig. 2. Underway ADCP velocity vectors, averaged over 54–102 m, with 10 minute time bins smoothed with an hourly running mean. Velocity vectors are coloured by surface water temperature, which is between 2 °C and 9 °C, in 0.5 °C intervals. The thermosalinograph measured water temperatures from an intake at approximately 5 m depth. Velocity values are indicated by the length of the lines, with a standard 1 m s^{-1} line shown at the top right of the figure. The lower figure shows the outward track along the North Scotia Ridge, while the upper figure shows the corresponding return track along the ridge to Shag Rocks Passage. Once Shag Rocks Passage was crossed on the return leg of the cruise, the ship took a direct route to the Falkland Islands rather than following the ridge. For this reason, only data for half of the return leg is presented here.

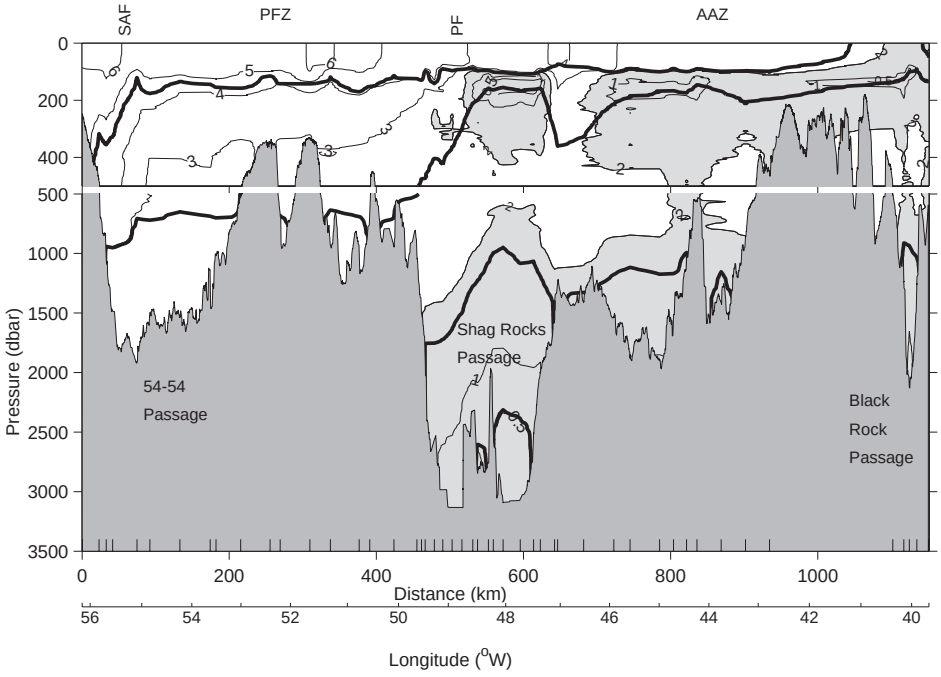

Fig. 3. Potential temperature section for the North Scotia Ridge. Values colder than 2°C are shaded grey. Dark lines denote water mass boundaries in neutral density, with values as defined in Fig. 5. The location of the Polar Front (PF) and Subantarctic Front (SAF) are marked, with the Polar Frontal Zone (PFZ) and Antarctic Zone (AAZ) indicated. Station locations are shown along the lower axis.

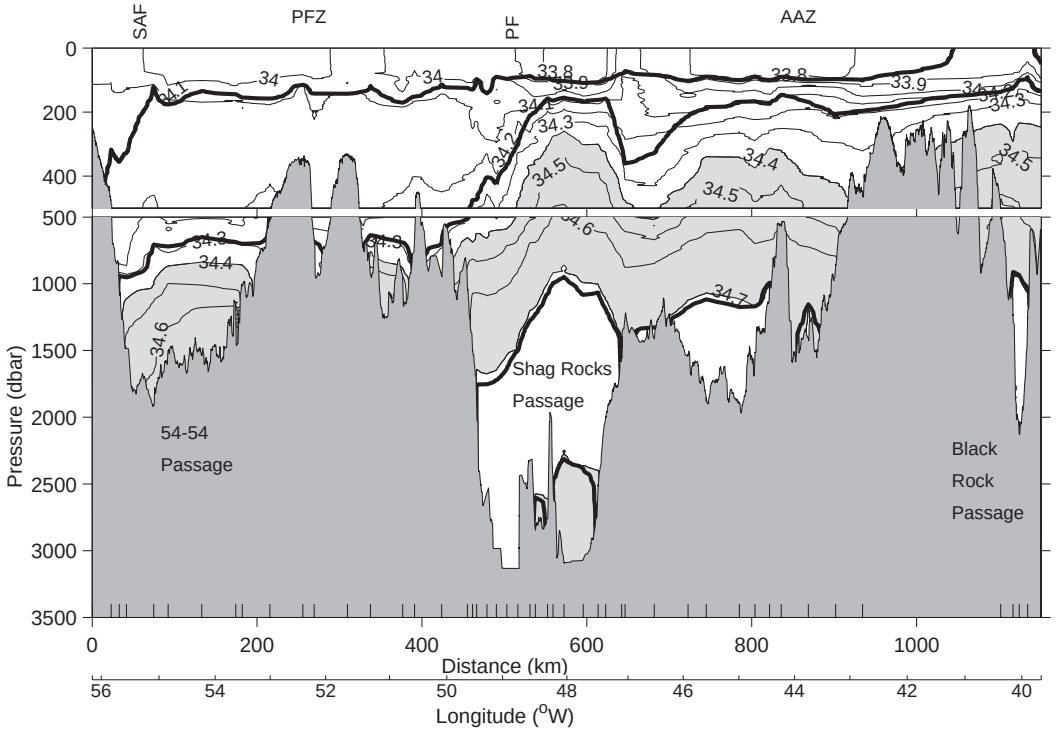

Fig. 4. Salinity section for the North Scotia Ridge. Dark lines denote water mass boundaries in neutral density, with values as defined in Fig. 5. Values between 34.4 and 34.7 are shaded grey. The location of the Polar Front (PF) and Subantarctic Front (SAF) are marked. Station locations are shown along the lower axis, with the Polar Frontal Zone (PFZ) and Antarctic Zone (AAZ) indicated.

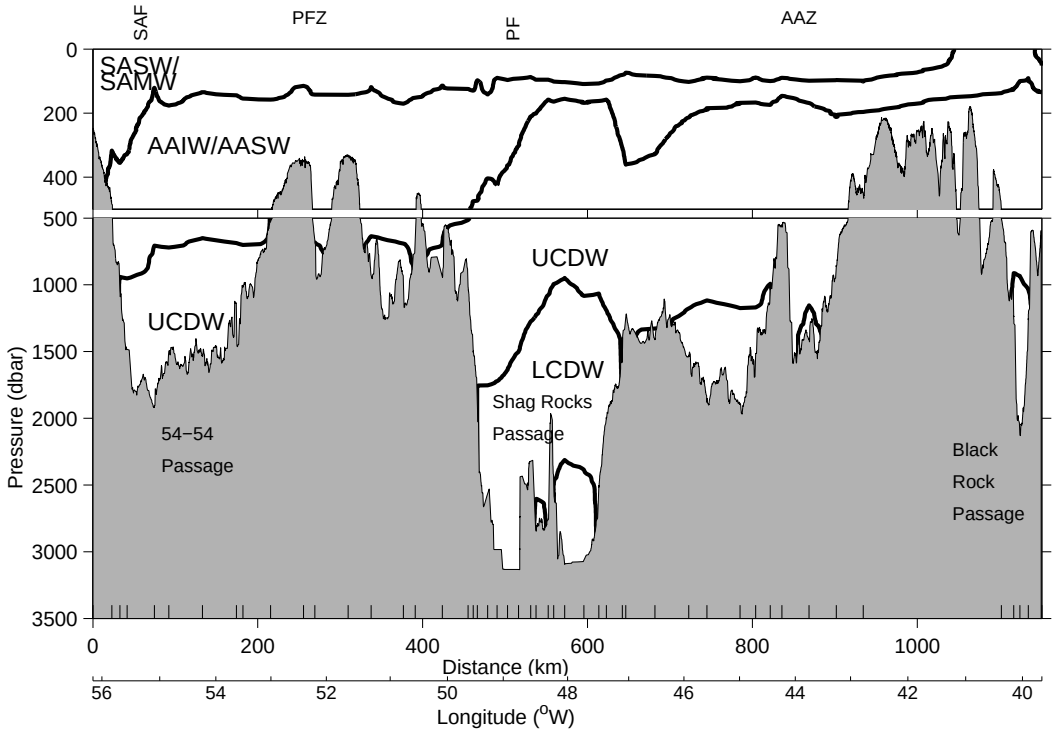

Fig. 5. Neutral density section defining the boundaries of water masses. Water masses with γ^n values less than 27.18 are denoted SASW/SAMW, while those with γ^n values between 27.18 and 27.55 are denoted AAIW/AASW. UCDW denotes waters with γ^n values between 27.55 and 28.00, while LCDW denotes waters with γ^n greater than 28.00. The boundary is also marked for γ^n values greater than 28.20, which is the nominal boundary for SPDW.

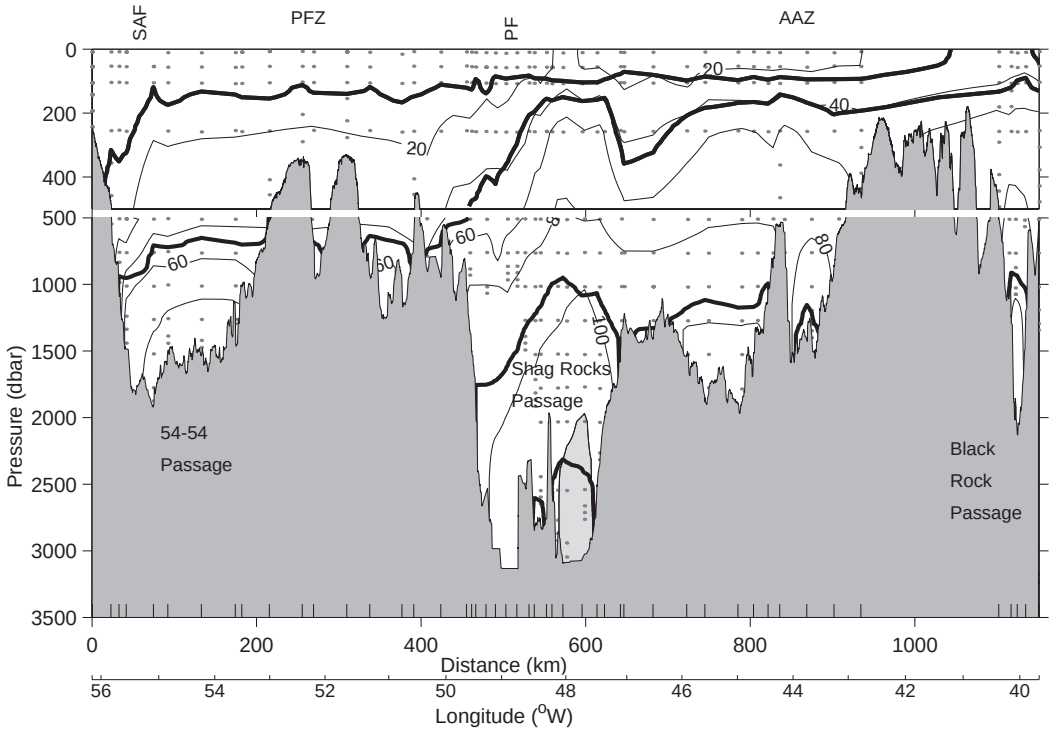

Fig. 6. Silicate section for the North Scotia Ridge. Dark lines denote water mass boundaries in neutral density, with values as defined in Fig. 5. Values with silicate values greater than 120 μmol kg^{-1} are shaded grey. The location of the Polar Front (PF) and Subantarctic Front (SAF) are marked, with the Polar Frontal Zone (PFZ) and Antarctic Zone (AAZ) indicated. Dots indicate the location of bottles used to construct the section. Station locations are shown along the lower axis.

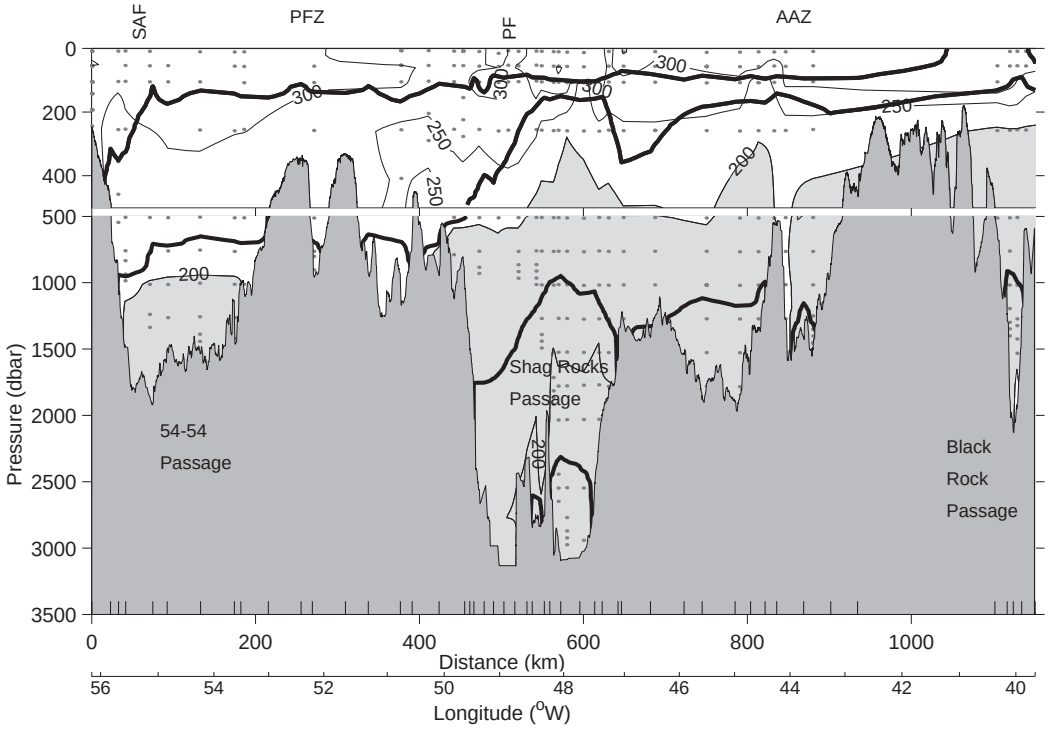

Fig. 7. Dissolved oxygen section for the North Scotia Ridge. Dark lines denote water mass boundaries in neutral density, with values as defined in Fig. 5. Values with oxygen values less than 200 μmol kg^{-1} are shaded grey. The location of the Polar Front (PF) and Subantarctic Front (SAF) are marked, with the Polar Frontal Zone (PFZ) and Antarctic Zone (AAZ) indicated. Dots indicate the location of bottles used to construct the section. Station locations are shown along the lower axis.

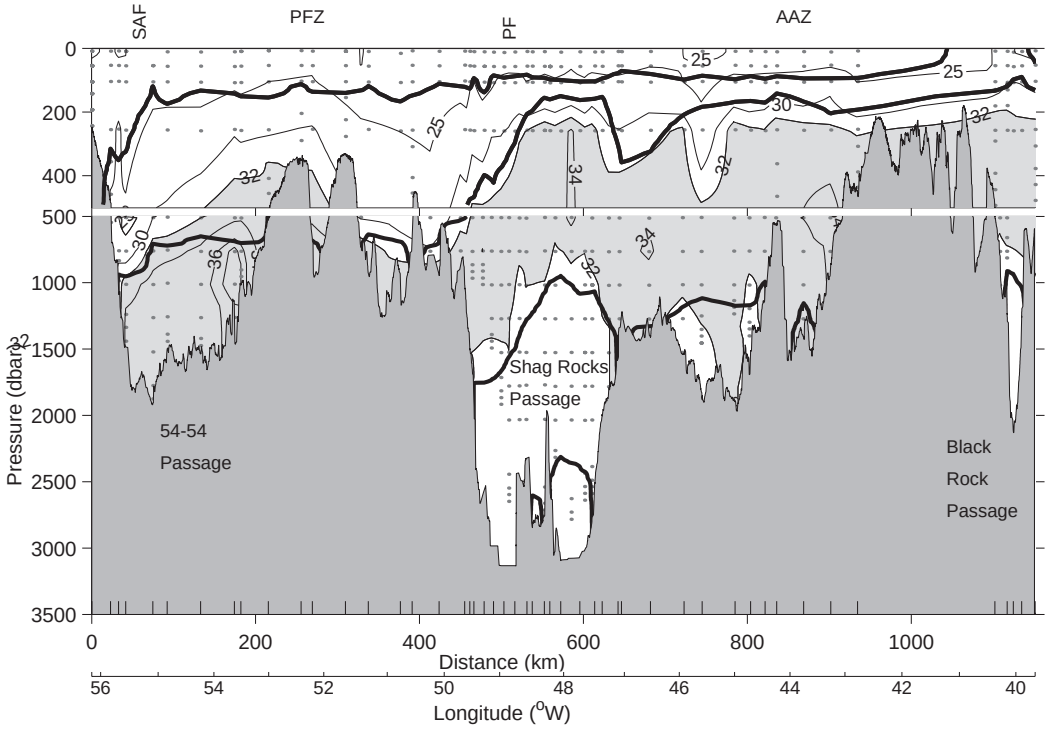

Fig. 8. Nitrate section for the North Scotia Ridge. Dark lines denote water mass boundaries in neutral density, with values as defined in Fig. 5. Values with nitrate values greater than 32 μmol kg^{-1} are shaded grey. The location of the Polar Front (PF) and Subantarctic Front (SAF) are marked, with the Polar Frontal Zone (PFZ) and Antarctic Zone (AAZ) indicated. Dots indicate the location of bottles used to construct the section. Station locations are shown along the lower axis.

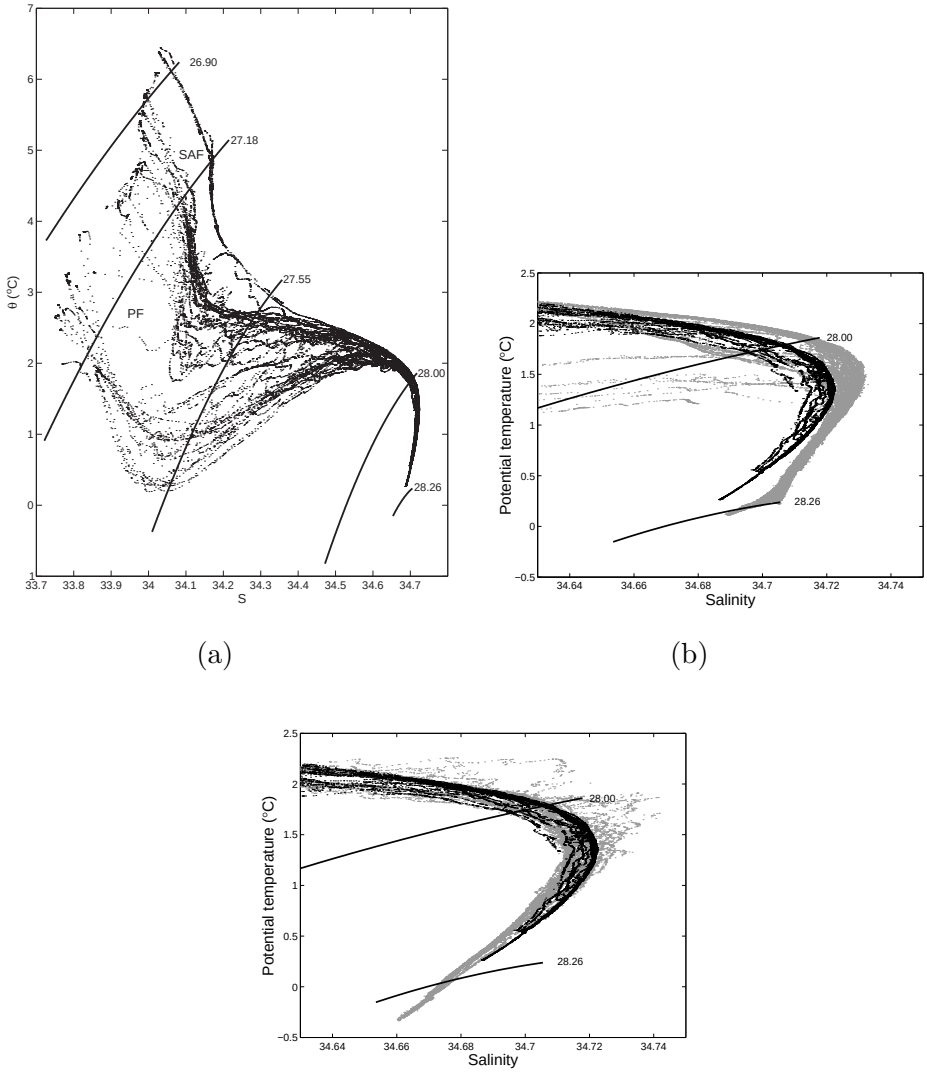

(a) (b)

(c)

Fig. 9. (a) Potential temperature versus salinity, for the 49 CTD stations occupied along the North Scotia Ridge (black dots). Voids in θ–S space mark the SAF and PF. Lines of neutral density (black lines, water mass separations) (Jackett and McDougall, 1997) are as for Fig. 5. (b) Close-up of densest water classes for the North Scotia Ridge (black dots) and for Drake Passage (grey dots - ALBATROSS cruise data from Naveira Garabato et al. (2002); stations for the ALBATROSS cruise are shown in Fig. 1). (c) Close-up of the densest water classes for the North Scotia Ridge (black dots) and for the Falkland Plateau/Georgia Basin (grey dots - ALBATROSS cruise data from Naveira Garabato et al. (2002); stations for the ALBATROSS cruise are shown in Fig. 1).

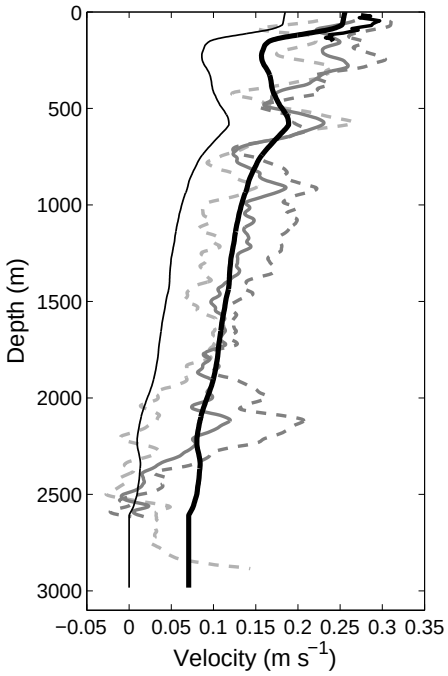

Fig. 10. Geostrophic shear for the pair of stations located at 49.1 °W and 48.9 °W, in Shag Rocks Passage. The thin black line is the geostrophic profile derived from CTD data, before any adjustments. The thick black line is the geostrophic profile adjusted by a constant offset based on the average value of the LADCP data. 150 kHz LADCP data are shown as grey broken lines. The darkest grey line is the mean of the corresponding light grey dashed (eastern station) and medium grey dashed (western station) lines. The short black solid line is the ship-mounted ADCP data to 150 m depth.

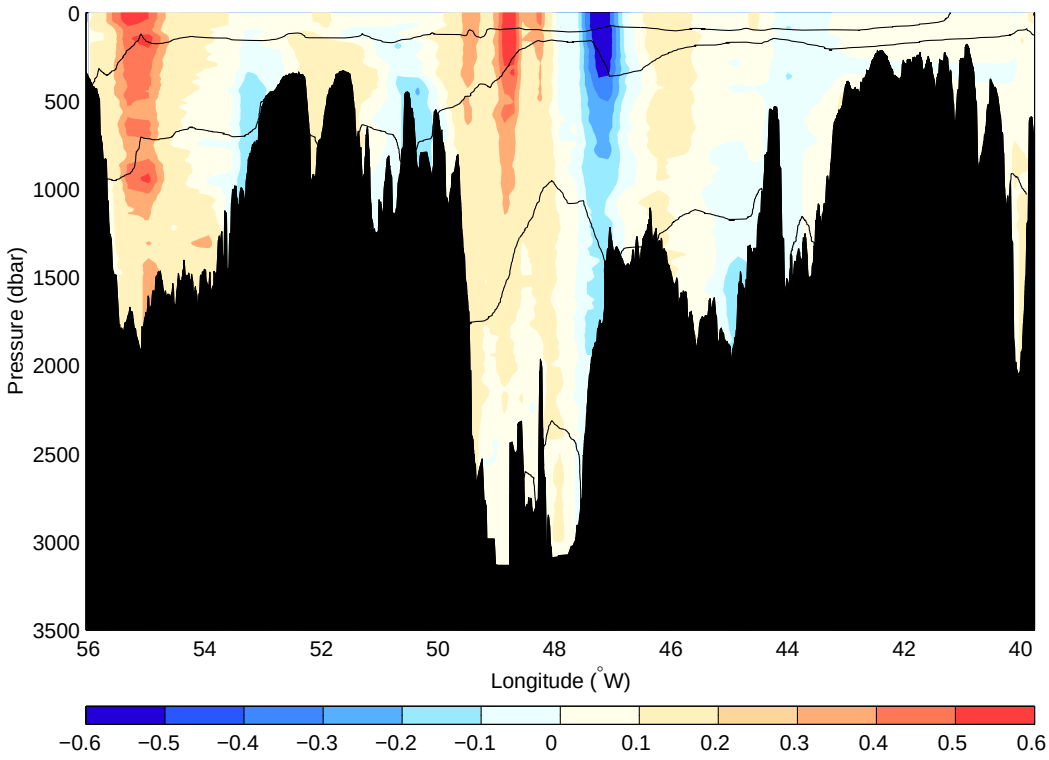

Fig. 11. LADCP velocity in m s^{-1} for station pairs along the North Scotia Ridge. Dark lines denote water mass boundaries in neutral density, with values as defined in Fig. 5.

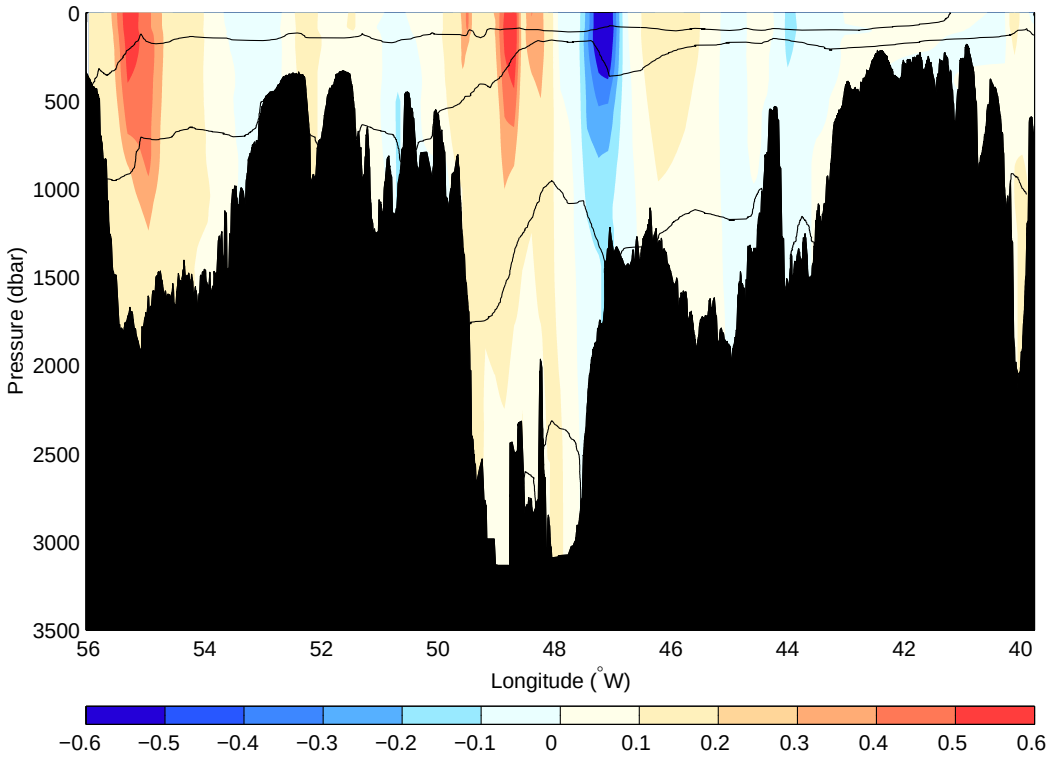

Fig. 12. Geostrophic velocity in m s^{-1} referenced to LADCP/ADCP profiles for station pairs along the North Scotia Ridge. Dark lines denote water mass boundaries in neutral density, with values as defined in Fig. 5.

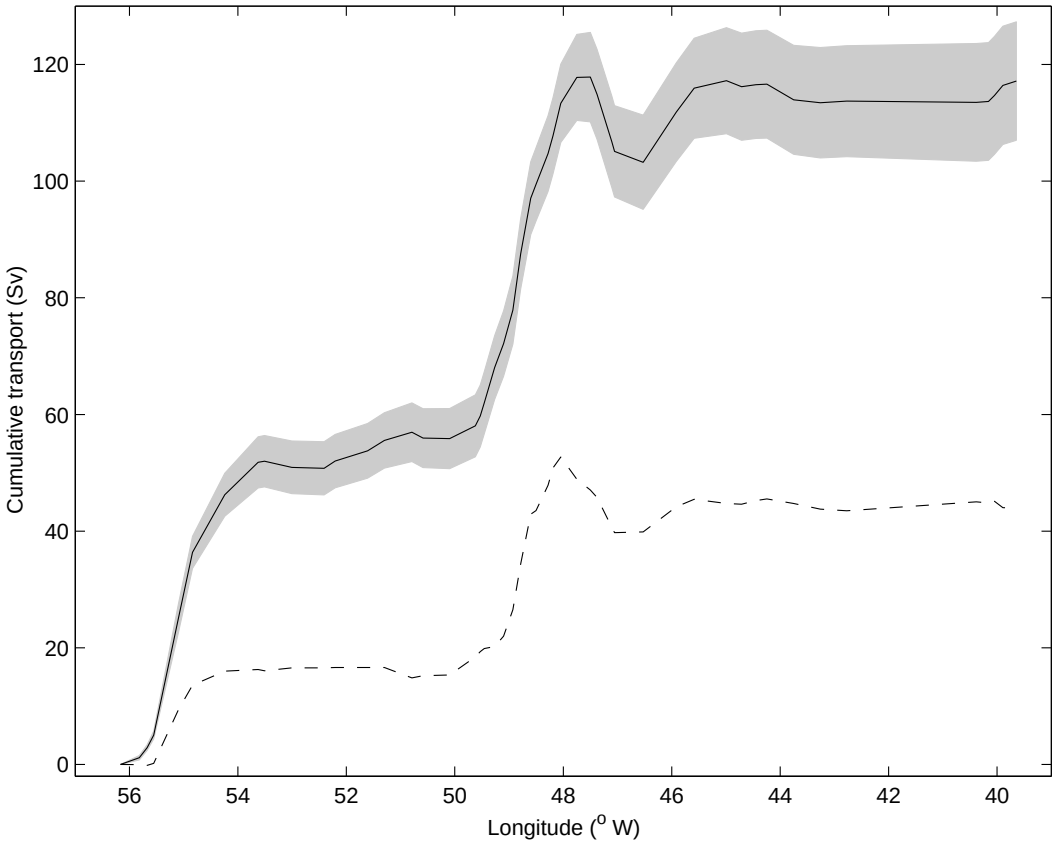

Fig. 13. Cumulative volume transports for NSROP. The solid line indicates the total net transport, obtained by referencing to LADCP/ADCP, while the dashed line denotes the baroclinic transport referenced to the deepest common level. Error bars for the total net transport were calculated from a Monte Carlo analysis and are shown as grey shading.

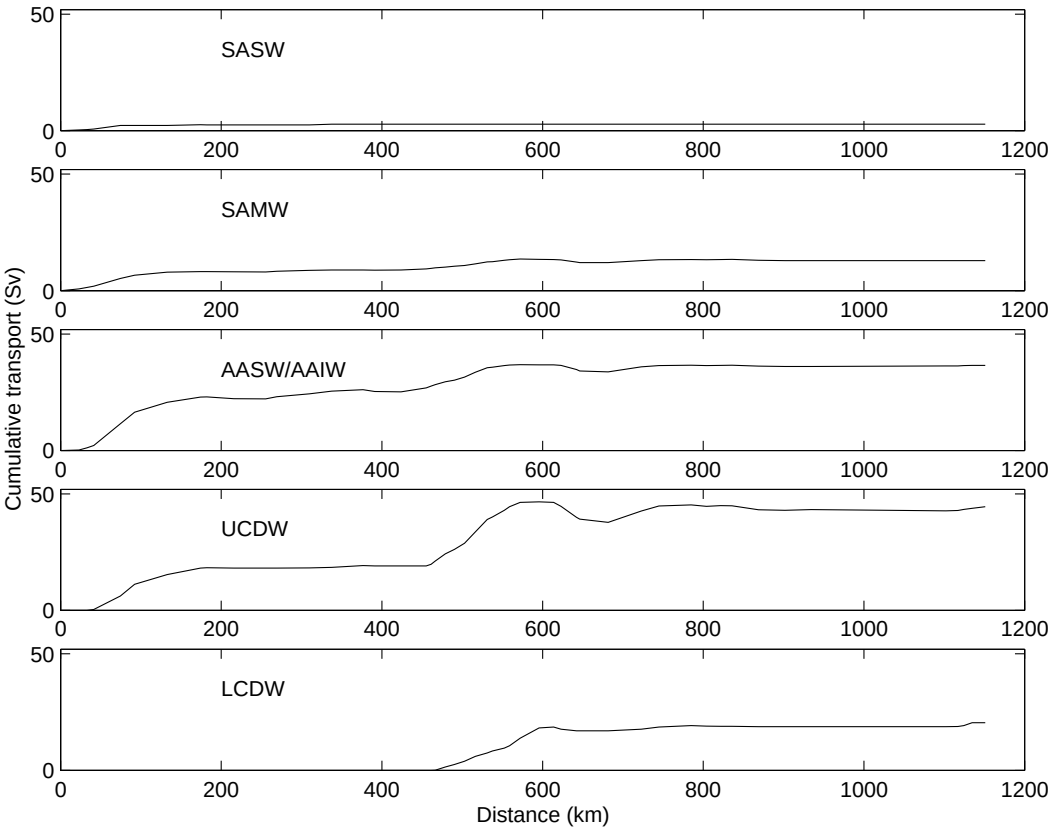

Fig. 14. Cumulative volume transports, accumulated from west to east, for water masses SASW, SAMW, AAIW/AASW, UCDW, and LCDW for the North Scotia Ridge.

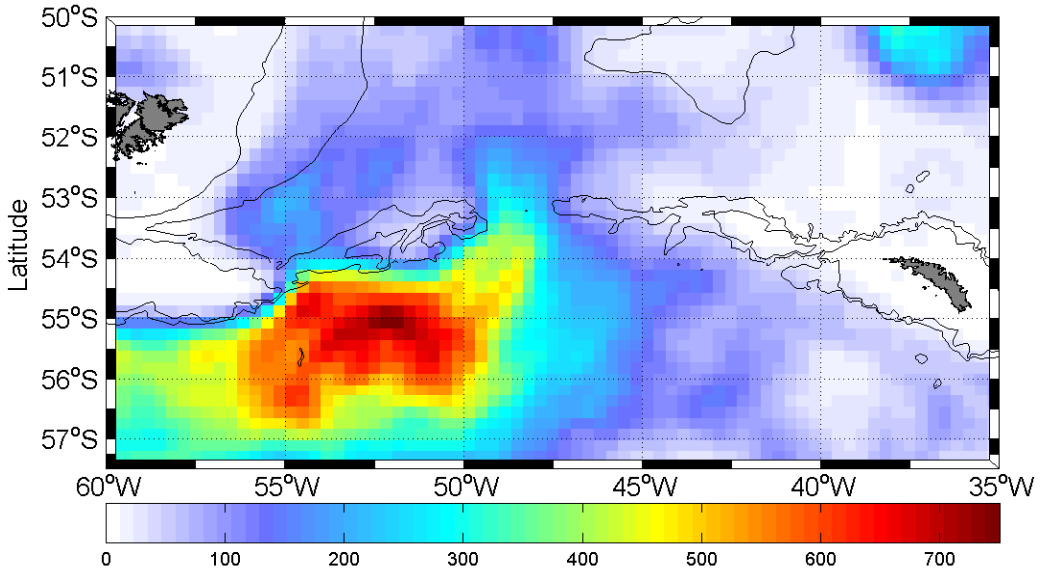

Fig. 15. Eddy Kinetic Energy (EKE) calculated from the AVISO joint TOPEX/ERS sea level anomaly product, covering the period 1992 to 2005. Units are cm^2s^{-2}.

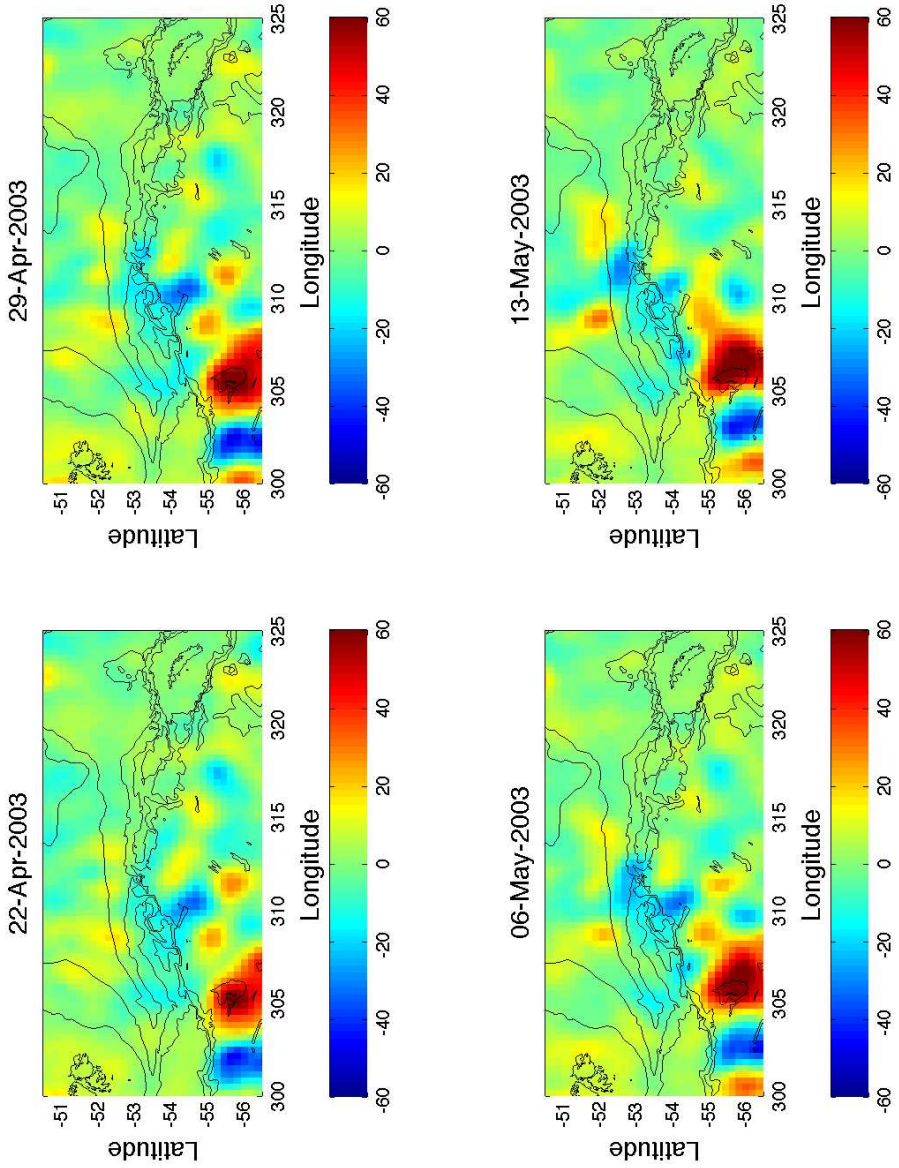

Fig. 16. Sequence of Sea Surface Height (SSH) anomalies spanning the time period of the cruise, specifically 22 April to 13 May 2003. Units are cm. Note in particular the negative SSH anomaly in the vicinity of Shag Rocks Passage during May 6-13, indicative of a cold-core (cyclonic) eddy present here at this time.